Potential X-Ray Production by RF Cavities in the HINS Linac Enclosure in the Meson Detector Building and Shielding Required for Safe Cavity Operation

Bob Webber

Revised January 27, 2009

Introduction

The Fermilab High Intensity Neutrino Source (HINS) R&D program will construct a shielding enclosure for the HINS 30 MeV proton/H- linac in the Meson Detector Building (MDB). The enclosure design must accommodate two potential radiation sources: 1) the loss and absorption of proton/H- ions during designed beam operations and 2) x-rays generated within the RF cavities even in the absence of the design beam.

This note addresses the second potential radiation source: x-rays due to electrons from ionized background gas or surface emission that are accelerated in the high electric fields of the RF cavities. Shielding requirements for radiation due to operation of the design proton or H- beam shall be documented elsewhere.

The linac comprises a Radio Frequency Quadrupole (RFQ), two copper-plated steel re-buncher RF cavities, sixteen copper (room temperature) RF accelerating cavities and eighteen β=0.2 SSR1 superconducting (SC) spoke resonator cavities. A conservative estimate of the x-rays potentially generated by operation of these cavities at their full design accelerating gradient is presented and corresponding shielding requirements are assessed.

Assumptions and Estimates

This document proceeds along the lines of logic used in “Estimate of X-Ray Shielding and Radiation Monitoring for Safe Operation of the HINS Cavity Test Cave in the Meson Detector Building”, Beams-doc 2598-v3.

Estimates of x-ray yields are based on the maximum energy that can be obtained by electrons emitted from the cavity surfaces, the power available to drive that electron current, and any physical factors that otherwise limit the electron current.

X-rays produced in the RFQ are not considered in this document. The RFQ is located outside the linac shielding enclosure and its construction includes a thick-wall steel vacuum vessel that provides attenuation for x-rays generated within the RF structure. X-ray measurements shall be made as the RFQ is commissioned to full RF power. Any required x-ray mitigations will be based on those measurements.

Table 1. Cavity Parameters

Cavity Type	Maximum Total Voltage	# of Gaps	Assumed Electron Beam Energy
Re-bunchers	0.165 MV	1	0.165 MeV
Copper 3-spoke	0.33 MV	2 full and 2 half	0.11 MeV
Copper 4-spoke	1 MV	3 full and 2 half	0.25 MeV
SC β=0.2	1.5 MV	2	0.75 MeV

Maximum Attainable Electron Energy Assumptions

All cavities to be operated in the HINS linac enclosure at MDB are designed for acceleration of non-relativistic protons or H- ions (e.g. β=0.2 for the SSR1 superconducting cavities). They are, by geometry, inherently ineffective for imparting the full, integrated multi-gap cavity voltage to particles of the "wrong" velocity. The large charge-to-mass ratio difference between protons and electrons makes the velocity of an electron "wrong" under any stable condition for these structures. It is reasonable to assume that the maximum possible energy imparted to an electron in the system is that from just one accelerating gap in a single cavity rather than that from the sum of multiple gaps. Table 1 shows the parameters used for x-ray shielding calculation purposes for each of the relevant cavity types.

Available RF Power

The HINS linac RF power distribution system is designed to supply a specific, individual level of power to each cavity determined by the cavity construction and the accelerator physics design of the linac. Tables 2 and 3 show the peak pulsed RF power required by each of the 16 copper cavities and the 18 superconducting cavities respectively. (Note that copper cavities 1-4 are the 3-spoke type and 5-16 are 4-spoke type.) The re-buncher cavities each require 6 kW RF power, well below that of the cavities that dominate the shielding requirements. The re-bunchers are considered no further.

The copper cavity table presents power requirements assuming 10 mA beam current, whereas the superconducting cavity table assumes 25 mA. For calculations in this document, the highest RF power level requirement for each cavity type is assumed, the copper cavity power is scaled up to that required for 25 mA beam current, and a 50% allowance for power overhead is applied. The assumed available operational peak power levels are then:

1.5*(10 + 25/10 * 2.14) = 23 kW for the Copper 3-spoke
1.5*(44 + 25/10 * 7.8) = 95 kW for the Copper 4-spoke
1.5*(32) = 48 kW for the SC β=0.2 cavity

Table 2. Copper Cavity Power Requirements*

2. Power consumption in the room temperature CH cavities.

Cavity number	design type	β geom.	β particle	Rsh MOhm	Veff MV	φ_s deg	dW MeV	W MeV	P_{copper} kW	P_{beam} kW	P_{total} kW
1	1	0.0744	0.0729	10.45	0.1807	-90	0.000	2.5	3.1246	0	3.1246
2	2	0.0771	0.0741	10.55	0.277	-50	0.178	2.678	7.2729	1.78	9.0529
3	3	0.0804	0.0767	10.994	0.2994	-50	0.192	2.871	8.1536	1.92	10.074
4	4	0.0842	0.0795	11.15	0.3336	-50	0.214	3.085	9.9811	2.14	12.121
5	5	0.0882	0.0825	15.64	0.3877	-50	0.249	3.334	9.6107	2.49	12.101
6	5	0.0882	0.0861	16.96	0.459	-45	0.325	3.659	12.422	3.25	15.672
7	8	0.1015	0.0905	14.38	0.5929	-45	0.419	4.078	24.446	4.19	28.636
8	8	0.1015	0.0955	17.16	0.6061	-40	0.464	4.542	21.408	4.64	26.048
9	8	0.1015	0.1008	18.62	0.6387	-35	0.523	5.065	21.909	5.23	27.139
10	11	0.116	0.1064	17.78	0.6983	-33	0.586	5.651	27.425	5.86	33.285
11	11	0.116	0.1121	19.77	0.7412	-33	0.622	6.273	27.788	6.22	34.008
12	11	0.116	0.1181	20.31	0.8216	-33	0.689	6.962	33.236	6.89	40.126
13	14	0.1316	0.1244	20.88	0.9425	-33	0.790	7.752	42.543	7.9	50.443
14	14	0.1316	0.1308	22.12	0.9071	-33	0.761	8.513	37.198	7.61	44.808
15	16	0.1422	0.1368	22.59	0.94	-33	0.788	9.301	39.115	7.88	46.995
16	16	0.1422	0.1426	23.29	1.0172	-40	0.779	10.081	44.427	7.79	52.217
								Total :	370.06	75.79	445.85

* from "Power tables for room temperature part of HINS", G. Romanov, Dec 29, 2008. (Assumes 10 ma proton beam for beam power calculation).

Table 3. Superconducting Spoke Cavity Power Requirements**

1			Cavity voltage (kV)	Beam power (kW) for 25 mA	phase (deg)
18	SSR-1	17	1168.96269	25.30878465	-30
19		18	1240.16921	26.85045103	-30
20		19	1300.11845	28.14839015	-30
21		20	1350.24307	29.23362001	-30
22		21	1388.20499	30.05551969	-30
23		22	1417.65869	30.693211	-30
24		23	1438.62264	31.14709383	-30
25		24	1454.30679	31.48666564	-30
26		25	1464.28768	31.70275824	-30
27		26	1471.59134	31.86088712	-30
28		27	1472.14355	31.87284282	-30
29		28	1472.62197	31.88320092	-30
30		29	1472.34967	31.87730545	-30
31		30	1470.75775	31.84283937	-30
32		31	1467.38566	31.76983148	-30
33		32	1461.86191	31.65023878	-30
34		33	1453.87773	31.47737622	-30
35		34	1448.63582	27.74298552	-40

** from "Ostroumov_energy_Nov_2006-revision-Feb_07.xls", Peter Ostroumov, February 2007. (Assumes 25 ma proton beam for beam power calculation).

A single 325 MHz, 2.5 MW peak power, pulsed klystron capable of a maximum 4.5 msec pulse and 1.5% duty factor drives the RF distribution system. Therefore, the time-averaged power available to any cavity is only 1.5% that of the peak value. The average power potentially available to drive x-ray production for each cavity type is:

345 W for the Copper 3-spoke
1429 W for the Copper 4-spoke
720 W for the SC β=0.2 cavity

Other Physical Factors

The production of x-rays from accelerated electrons is an inefficient process; at energies of concern here, >90% of the electron power becomes heat in the x-ray producing target [1] [Appendix 1]. In the superconducting cavities, heat due to the wasted electron power not converted to x-rays must be removed by the cryogenic system. That system is designed to remove only a few tens of watts from any cavity while maintaining it at superconducting temperature and thereby allowing operation at design accelerating field. Calculations in this paper take no credit for this limiting effect and assume that SC cavity operation in the presence of 720 W of electron power is possible. This renders the subsequent analysis results conservative by at least a factor of ten.

X-ray shielding provided by the ½ inch stainless steel wall of the cryomodule that houses the SC cavities is neglected in the calculations. This provides an additional factor-of-two conservatism to the analysis.

X-Ray Source Term and Shielding Calculations

Based on the parameters described above and assuming that the entire average RF power is available to produce electrons of the specified energy, the electron current available for x-ray production from each cavity type is:

Copper 3-spoke --- 345 W / 0.11 MV = 3.2 mA
Copper 4-spoke --- 1429W / 0.25 MV = 5.7 mA
SC β=0.2 cavity --- 720 W / 0.75 MV = 1.0 mA

The corresponding absorbed dose rates D for x-rays at one meter from an x-ray producing target are obtained from graph E.1 in NCRP Report No.51.

For copper 3-spoke cavity
At 0° $D = <0.5$ (rad m$^{2)}$ / (min mA) x 3.2 mA = < 1.5 rad m^2/min
At 90° $D = <1$ (rad m$^{2)}$ / (min mA) x 3.2 mA = < 3.2 rad m^2/min

For copper 4-spoke cavity
At 0° $D = <0.5$ (rad m$^{2)}$ / (min mA) x 5.7 mA = < 2.9 rad m^2/min
At 90° $D = \sim 1$ (rad m$^{2)}$ / (min mA) x 5.7 mA = ~5.7 rad m^2/min

For SC β=0.2 cavity

At 0° D = 8 (rad m$^{2)}$ / (min mA) x 1.0 mA = 8 rad m^2/min

At 90° D = 20 (rad m$^{2)}$ / (min mA) x 1.0 mA = 20 rad m^2/min

The dose calculations that follow assume the most demanding case, SC cavities each presenting a radiation source term:

SC β=0.2 cavity at 90° D = 20 rad m^2/min = 1.2E6 mrad m^2/hr

Figure 1 shows the enclosure cross-section in the region of the SC cavities. The ceiling height of the enclosure is 10.5 feet, in which case, the building crane height limits the enclosure roof thickness to three feet. With a cavity centerline height of 50.6 inches, the distance to the top of the roof is 111.4 inches or 2.83 meters. The enclosure sidewalls are farther from the cavity centerline than is the ceiling and the sidewalls offer the possibility of more than three feet shielding thickness if required. Therefore, the pertinent reference point for calculating potential radiation dose from the cavities is on the rooftop.

In the linac, there are 18 SC cavities distributed in two cryomodules with a typical cavity-to-cavity spacing of 0.75 meters. Figure 2 shows the configuration. The total potential dose at a reference point on the rooftop above the line of cavities is the sum of that from each cavity with the respective distance and shielding factors taken into account.

The unshielded dose rate from a reference cavity immediately below the reference point is:

$$D_{0\text{unsh}} = \text{D} / d^2 = 1.2\text{E}6 / 2.83^2 = 1.5\text{E}5 \text{ mrad/hr}$$

Figure E.12 in NCRP Report 51 gives the shielding dose equivalent tenth-value layer (TVL) thickness for x-rays in concrete as a function of primary electron beam energy. For 0.75 MeV electrons, the first tenth-value layer is ~7 inches and subsequent layers are

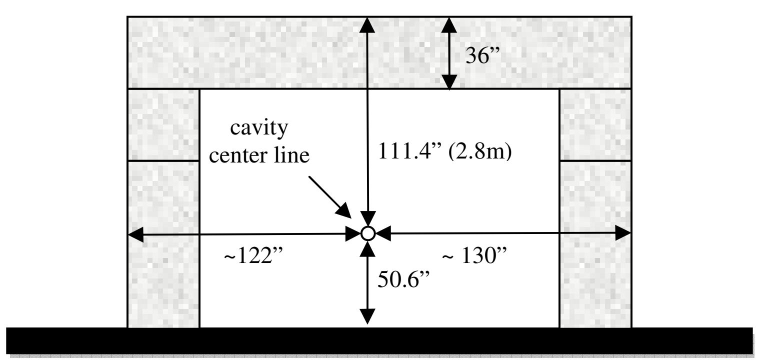

Figure

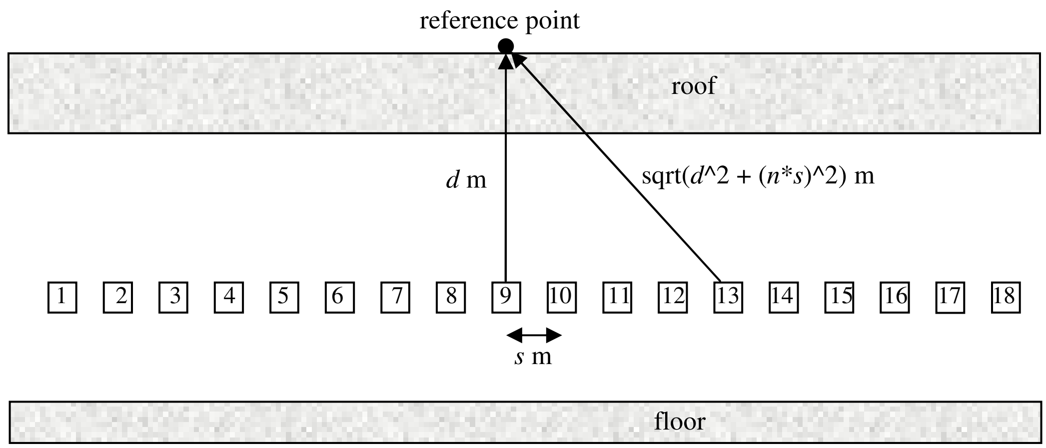

Figure 2. Superconducting Cavity Layout Geometry

each ~5 inches. It follows that concrete shielding of thickness *th* inches then represents 1 + (*th* - 7)/5 tenth-value layers, provided *th* > 7.

The reference-point dose rate from the reference cavity with 36-inch roof thickness is then:

$$D_{0s} = D_{0unsh} / 1E(\#TVLs) = 1.5E5 / 1E(1 + (36-7)/5) = 0.024 \text{ mrad/hr}$$

Two factors reduce the reference-point dose rate contribution from cavities on either side of the reference cavity; the 'reference point to source' separation is greater and the effective shielding thickness is greater. As depicted in Figure 2, the relevant distance for a cavity *n* positions from the reference cavity is:

$$dn = \text{sqrt}(d^2 + (n*s)^2)$$

and the effective shielding thickness is:

$$thn = th * dn / d$$

Therefore, the unshielded dose from a cavity *n* positions from the reference is:

$$Dn_{unsh} = \mathrm{D} / (d^2 + (n*s)^2)$$

The transmission through the shielding from this cavity to the reference point is:

$$Tn = 1 / 1E(\ 1+ ((th*dn/d)-7) / 5)\ )$$

And finally, the resulting reference point shielded dose from that cavity is:

$$Dn_s = Dn_{unsh} * Tn$$

Table 4. Geometry Effects for Radiation from Cavities Offset from Reference

A	B	C	D	E
0	3	1	1	0.024
1	3.104	0.934	0.564	0.013
2	3.395	0.781	0.112	$2.086 \cdot 10^{-3}$
3	3.833	0.613	0.01	$1.461 \cdot 10^{-4}$
4	4.372	0.471	$5.098 \cdot 10^{-4}$	$5.7 \cdot 10^{-6}$
5	4.98	0.363	$1.768 \cdot 10^{-5}$	$1.523 \cdot 10^{-7}$
6	5.635	0.283	$4.736 \cdot 10^{-7}$	$3.187 \cdot 10^{-9}$
7	6.322	0.225	$1.062 \cdot 10^{-8}$	$5.678 \cdot 10^{-11}$
8	7.032	0.182	$2.1 \cdot 10^{-10}$	$9.074 \cdot 10^{-13}$
9	7.759	0.149	$3.79 \cdot 10^{-12}$	$1.345 \cdot 10^{-14}$

A = *n*, cavity offset position (0 equals reference cavity)
B = *thn*, distance to dose reference point (meters)
C = $Dn_{\text{unsh}} / D0_{\text{unsh}}$,1/d^2 dose factor relative to reference cavity
D = Tn/T_0, shielding transmission factor relative to reference cavity
E = Dn_s, dose contribution at reference point (mr/hr)

Table 4 displays the values of these terms for the geometry of Figure 2. The table shows that the increased shielding thickness due to the ‘hypotenuse effect’ is more important than the 1/d^2 distance effect for reducing dose from offset cavities. This shielding effect renders radiation from offset cavities insignificant for any cavities offset from the reference by more than three positions.

Analytically, the rooftop dose at the center of a line of 2*k*+1 cavities is:

$$D_{2k+1} = D \cdot \left(-\frac{10^{-(1+(th-7)/5)}}{d^2} + 2 \cdot \sum_{n=0}^{k} \frac{10^{-(1+((th*dn/d)-7)/5)}}{d^2 + (n \cdot s)^2} \right) \text{ rad/min}$$

With d=2.8 m, s=0.75 m and conservatively taking the summation over k=9, the quantity D_{2k+1} is found to be 0.053 mrad/hr.

This is in agreement with the result obtained by adding the doses shown in Table 4, Column E, from the reference cavity and three cavities upstream and downstream.

Conclusion

Calculations show that radiation due to RF cavity-produced x-ray outside the HINS linac enclosure will be small if that enclosure is constructed with concrete walls and roof at least three feet thick. Even neglecting realistic cryogenic system heat removal limitations and x-ray shielding offered by the SC cavity cryomodule walls, the worst case dose outside the enclosure due to RF cavity-produced x-rays is calculated to be of order 0.05 mr/hr.

References

1. Evans, Robley D., "The Atomic Nucleus", McGraw-Hill, 1955, pp. 609-610.

Appendix 1. From "The Atomic Nucleus", Robley D. Evans

with Webber notations

THE ATOMIC NUCLEUS

Robley D. Evans, Ph.D.
PROFESSOR OF PHYSICS
MASSACHUSETTS INSTITUTE OF TECHNOLOGY

New York Toronto London
McGRAW-HILL BOOK COMPANY, INC.
1955

The actual path of an electron while passing through an absorbing foil is not straight. Because of the effects of multiple scattering, the actual path length is always greater than the foil thickness traversed. The ratio of the actual path length to the superficial thickness of absorber traversed increases with Z (Chap. 21, Sec. 1). In the case of electrons (but not heavy particles), the effect of scattering almost exactly balances the decrease of dT/dw with increasing Z. Therefore, if distance is measured in terms of superficial thickness of absorber traversed, say, in milligrams per square centimeter, the ionization losses for positrons and

Note: this discussion assumes thin targets

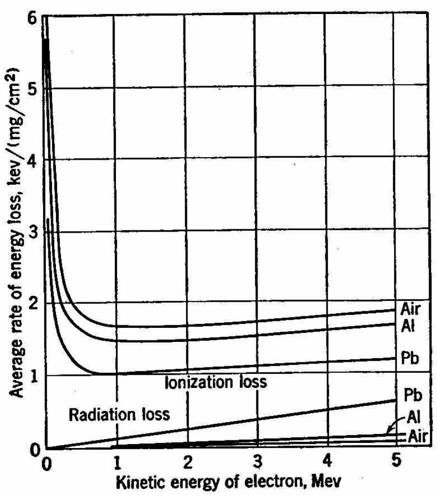

Fig. 2.1 Mass-absorption energy losses for electrons in air, Al, and Pb. The upper three curves are $(dT/dw)_{\text{ion}}$, based on Eq. (2.26) of Chap. 18, with $dw = \rho\, ds$, and $I_{\text{air}} = 86$ ev, $I_{\text{Al}} = 165$ ev, $I_{\text{Pb}} = 750$ ev. The three lower curves show, on the same scales, the average energy loss due to bremsstrahlung $(dT/dw)_{\text{rad}}$ as obtained from Eq. (1.9), with $dw = \rho\, ds$. All curves refer to energy losses along the actual path traversed by the electron.

negatrons become nearly independent of the nature of the absorbing material. It is therefore common in reporting experimental work to use milligrams per square centimeter, or a similar unit, as the measure of absorber thickness.

c. Ratio of Radiative and Ionization Losses. Ionization losses per unit path length vary roughly as $1/\beta^2$ and so are largest for slow particles. On the other hand, radiative losses increase with increasing energy, Eq. (1.9). At high energies, $T \gg Mc^2$ in general, or $T \gg m_0c^2$ for electrons, the radiative losses become comparable with the ionization losses.

The ratio of the radiative to the ionization losses, for any particle of rest mass M_0, and high velocity $\beta \simeq 1$, is obtainable from the quotient of Eq. (1.9) and Eq. (2.26) of Chap. 18. With $137\sigma_0$ generalized to

$(e^2/M_0c^2)^2$, the ratio becomes approximately (B55)

$$\frac{(dT/ds)_{\text{rad}}}{(dT/ds)_{\text{ion}}} \simeq Z\left(\frac{m_0}{M_0}\right)^2\left(\frac{T}{1{,}600m_0c^2}\right) \tag{2.8}$$

The factor 1,600 holds for electrons ($M_0 = m_0$) but should be reduced to about 1,000 for mesons ($M_0 \sim 200m_0$). Thus we see that, for electrons, the radiative and ionization losses are equal for $T = 20m_0c^2 = 10$ Mev in Pb (and for $T \sim 100$ Mev in water or air).

The numerical values of σ_{rad} are such that *for electrons at* 10 *Mev the radiative and ionization losses are each equal to about* 1.6 *Mev per millimeter of* Pb, or a total of 3.2 Mev per millimeter of Pb for both. This makes a very convenient rule of thumb for estimating high-energy radiative losses (which increase approximately with NZ^2 and T) and ionization losses (which increase with NZ but are nearly independent of T).

So for example
with 3 MeV electrons on iron
$Z = 26$

$$\frac{\left(\frac{dT}{ds}\right)_{\text{RAD}}}{\left(\frac{dT}{ds}\right)_{\text{ION}}} = 26\left(\frac{1}{1}\right)^2\left(\frac{T = 3\text{ MeV}}{1600\left(\frac{1}{2}\text{ MeV}\right)}\right)$$

$$= \frac{26 \cdot 3}{1600/2} \simeq \frac{78}{800} \simeq 10\%$$

So at 3 MeV only 10% of electron energy is converted to photons, 90% goes to ionization and therefore to heat in target

For thick targets (series of thin targets w/ ever decreasing electron energy) photon yield is lower yet.